TITLE: Cryopreservation of canine cardiosphere-derived cells: Implications for clinical application

AUTHORS: Dutton, L. C., Church, S. A.V., Hodgkiss-Geere, H., Catchpole, B., Huggins, A., Dudhia, J. and Connolly, D. J.

JOURNAL: Cytometry Part A

PUBLISHER: Wiley

PUBLICATION DATE: January 2018

DOI: 10.1002/cyto.a.23186

Cryopreservation of canine cardiosphere-derived cells: implications for clinical application

Luke C. Dutton[1, 4]

Sophie A.V. Church[1] Hannah Hodgkiss-Geere[2] Brian Catchpole[3] Anthony Huggins[3]

Jayesh Dudhia[1, 5]

David J. Connolly[1, 5]

[1]Department of Clinical Science and Services, Royal Veterinary College, University of London, United Kingdom

[2]Department of Veterinary Clinical Science, University of Liverpool, United Kingdom

[3]Department of Pathobiology and Population Sciences, Royal Veterinary College, University of London, United Kingdom

[4]Correspondance to: Luke C. Dutton, Clinical Science and Services, Royal Veterinary College, Hawkshead Lane, North Mymms, Hatfield, Herts AL9 7TA, UK. E-mail: lcdutton@rvc.ac.uk

[5]Senior authors

Abstract

The clinical application of cardiosphere-derived cells (CDCs) to treat cardiac disease has gained increasing interest over the past decade. Recent clinical trials confirm their regenerative capabilities, although much remains to be elucidated about their basic biology. To develop this new treatment modality, in a cost effective and standardised workflow, necessitates the creation of cryopreserved cell lines to facilitate access for cardiac patients requiring urgent therapy. Cryopreservation may however lead to alterations in cell behaviour and potency. The aim of this study was to investigate the effect of cryopreservation on canine CDCs. CDCs and mesenchymal stem cells (MSCs) isolated from five dogs were characterized. CDCs demonstrated a population doubling time that was unchanged by cryopreservation (fresh versus cryopreserved; 57.13 ± 5.27 h versus 48.94 ± 9.55 h, $P = 0.71$). This was slower than for MSCs (30.46 h, $P < 0.05$). The ability to form clones, self-renew and commit to multiple lineages was unaffected by cryopreservation. Cryopreserved CDCs formed larger cardiospheres compared to fresh cells ($P < 0.0001$). Fresh CDCs showed a high proportion of $CD105^+$ (89.0% ± 4.98) and $CD44^+$ (99.68% ± 0.13) cells with varying proportions of $CD90^+$ (23.36% ± 9.78), $CD34^+$ (7.18% ± 4.03) and c-Kit^+ (13.17% ± 8.67) cells. $CD45^+$ (0.015% ± 0.005) and $CD29^+$ (2.92% ± 2.46) populations were negligible. Increasing passage number of fresh CDCs correlated with an increase in the proportion of $CD34^+$ and a decrease in $CD90^+$ cells ($P = 0.003$ and 0.03 respectively). Cryopreserved CDCs displayed increased $CD34^+$ ($P < 0.001$) and

decreased $CD90^+$ cells ($P = 0.042$) when compared to fresh cells. Overall, our study shows that cryopreservation of canine CDCs is feasible without altering their stem characteristics, thereby facilitating their utilisation for clinical trials.

Key Terms

Cardiosphere-derived cells; canine; cryopreservation; differentiation; stem cells

Introduction

Non-ischemic dilated cardiomyopathy (DCM) is the second most common cardiac disease of dogs, accounting for 10% of canine cardiac diagnoses (1). DCM is a heterogeneous disease of the canine myocardium that demonstrates breed specific characteristics at pathological and clinical levels (2). An underlying genetic basis has been proposed in a number of breeds, including the Doberman and Boxer, where the disease has been studied in detail and shown to be both common and severe with a cumulative prevalence in European Dobermans >8 years of age of 44% (2–7). Two distinct histopathological variations of canine DCM have been described; attenuated wavy fibre type and fibro-fatty infiltration type (7). Fibro-fatty infiltration is considered analogous to arrhythmogenic right ventricular cardiomyopathy (ARVC) in humans because of the comparable pathological changes and clinical presentation between the two species (8–12). Although the pathophysiologic mechanism underlying ARVC remains unclear, it is thought to include molecular pathways involved in the formation of mechanical and electrical coupling, apoptosis, and migration and differentiation of epicardial-derived cells (13). The electrical uncoupling together with fibro-fatty replacement of the myocardium are considered primary substrates for arrhythmia and sudden cardiac death is a frequent consequence (10). Dogs that survive develop progressive ventricular dilation and systolic dysfunction leading to congestive heart failure (12,14). Similar to humans, treatment options are limited and directed towards controlling clinical signs but do not promote myocardial repair or ultimately reduce disease progression.

Since the discovery that the adult heart had regenerative ability there has been increasing interest in the therapeutic use of adult cardiac stem cells (15,16). Multiple populations of cardiac progenitor cells have been isolated, such as side population cells, stem-cell antigen positive cells (Sca-1$^+$), c-Kit$^+$ (also known as CD117) cells, Islet-1$^+$ cells, cardiospheres and cardiosphere-derived cells (CDCs) (17–23). CDCs in particular have drawn much attention since there is mounting evidence they contribute to myocardial repair (22,24–27). Phase 1 clinical trials in humans have shown improved cardiac function using autologous CDCs (28,29). Allogeneic CDC therapy was shown to be safe, with marginal improvement in cardiac function, in a small clinical trial in Dobermans with DCM; however, there was no increase in survival time (30).

CDCs represent a heterogeneous cardiac stem cell population with the ability to form clones, self-renew and commit to multiple lineages including smooth muscle, myocardium and endothelium (25,31,32). CDCs are isolated from an intermediate cell population of cardiospheres which have been generated using various methods, including plating of cardiac outgrowth cells on poly-D-lysine coated wells (21,33), the use of forced aggregation on low attachment surfaces (25,30), aggregation plates and the hanging drop method (32). Cardiospheres are then cultured on plastic to form a monolayer of CDCs, which can be readily passaged and expanded to clinically useful cell numbers (28).

The development of a cost effective and efficient clinical treatment would necessitate the creation of cell banks for allogeneic applications, where cardiac stem cells from donor dogs could be cultured, characterised, assessed for endotoxins, purity and subsequently

cryopreserved. The aim of this work was to investigate the immunophenotype and basic cellular characteristics of canine CDCs prior to and following cryopreservation.

Materials and Methods

Tissue preparation

Canine tissue was obtained immediately post-mortem from five cadavers with owners' informed consent following approval by the Royal Veterinary College Ethics and Welfare Committee (Approval number: URN 2013 1246). Donors were aged 0.5, 4, 5, 5 and 6 years. Full thickness atrial tissue was aseptically removed and placed in chilled cardiac explant medium (CEM) consisting of Iscove's Modified Dulbecco's Medium (IMDM), 10% foetal bovine serum (FBS), 1% L-glutamine, 1% penicillin-streptomycin (P/S) (all from Thermo Fisher Scientific) and 0.1 mmol/L 2-mercaptoethanol (2-ME) (Sigma-Aldrich). Subcutaneous adipose tissue was harvested from the popliteal region and placed in mesenchymal stem cell media (MSCM) consisting of high glucose (4.5 g/L) Dulbecco's Modified Eagle's Medium (DMEM) (Thermo Fisher Scientific) supplemented with 10% FBS and 1% P/S.

Preparation of Cardiosphere-derived Cells

Atrial tissue was minced into <1 mm^3 explants and washed with Dulbecco's Phosphate-Buffered Saline (DPBS) (Thermo Fisher Scientific). The explants were digested in 0.2% trypsin and 0.1% collagenase IV (both from Thermo Fisher Scientific) three times for 5 min each at 37°C. After the final digestion, explants were placed in 5 mL of CEM for 5 min and then transferred onto fibronectin (Thermo Fisher Scientific) coated 25 cm^2 tissue culture flasks (Greiner Bio One) with 2-3 explants per flask. These were allowed to adhere for 30-60 min, after which 5-7 mL of CEM media was added and incubated in standard tissue culture conditions (37°C and 5% CO_2 in humidified air) to allow a stromal-like cell

layer to emerge as an outgrowth from the explants over a period of 3-7 days, during which time phase-bright cells appeared above the cell monolayer (21,31,33). Cells were detached with TrypLE Express (Thermo Fisher Scientific) and plated at a density of 1 x 10^5/cm^2 on Ultra-Low Attachment flasks (ULA) (Corning) in CEM containing 10% FBS. Once cardiospheres had formed over 5-7 days, they were collected and seeded onto fibronectin coated flasks to yield cardiosphere-derived cells (CDCs) in CEM with 20% FBS. Cells were passaged at 60-80% confluence by washing twice with DPBS and incubating with 0.25% trypsin (Thermo Fisher Scientific) for 5 min in tissue culture conditions. Trypsin was inactivated by adding an equal volume of CEM and cells centrifuged at 400*g* for 7 min. CDCs were cryopreserved in CellBanker 2 medium (AMS Biotechnology Ltd.) at a density of 1-2 x 10^6/mL and temperature decrease of -1°C/min in a freezing container (Mr Frosty, Thermo Fisher Scientific) to -80°C. CDCs were transferred to liquid nitrogen storage after 24 h.

Preparation of Mesenchymal Stem Cells

Canine adipose-derived mesenchymal stem cells (MSCs) were isolated as previously described (34–36). This cell type was used for comparison since they can be readily obtained, cultured and is the most comprehensively characterized canine adult stem cell. Briefly, tissue samples were washed twice with 5 mL of DPBS, finely minced with scissors and then incubated with 0.2% collagenase IV at 37°C with mild agitation (40 rpm) for 45 min. The resulting suspension was filtered through a 70μm nylon cell strainer (Corning) and centrifuged at 1,000*g* for 10 min. The supernatant was discarded and the cell pellet

re-suspended in 1 mL of MSCM. Cells were counted by Trypan blue (Sigma-Aldrich) dye exclusion and seeded onto 25 cm^2 tissue culture flasks at a density of 3-5 x 10^4 cells/cm^2. These were incubated in tissue culture conditions. After 24 h unattached cells were removed with two DPBS washes. Cells were passaged and cryopreserved as described for CDCs. Both fresh and cryopreserved MSCs were used for analysis, since cryopreservation has been shown to not alter their stem characteristics (37).

Cellular assays were performed on at least three donor (biological) samples with three technical replicates for each donor sample.

Antibody staining for flow cytometry

Cryopreserved cells were rapidly thawed at 37°C, re-suspended in appropriate growth media, washed once by centrifugation at 400*g* for 7 min and cultured in the same conditions as fresh cells for 3-5 days prior to antibody staining. Fresh cells were used directly from tissue culture vessels. Cells were detached by washing twice with DPBS and incubating at 37°C with Accutase (Thermo Fisher Scientific). Recovered cells were pelleted by centrifugation (400*g* for 5 min at 20°C), pellets were washed with chilled (4°C) FACS buffer (FACSFlow; BD Biosciences), re-suspended at a concentration of 3 x 10^6/mL in FACS buffer and 100µL aliquots transferred into FACS tubes (Thermo Fisher Scientific). Monoclonal antibodies or isotope-matched controls were added to each tube and incubated for 30 min at 4°C protected from light. Cells were pelleted by centrifugation at 400*g* for 5 min at 4°C, washed by re-suspension in FACS buffer and suspended in 1 mL of FACS buffer for acquisition. The antibodies used were anti-canine CD90 (eBioscience,

clone YKIX337.217, 1:20 dilution), anti-mouse CD105 (BD Biosciences, clone MJ7/18, 1:10), anti-human CD44 (Biolegend, clone IM7, 1:20), anti-human CD29 (BD Bioscience, clone MAR4, 1:20), anti-canine CD34 (R&D Systems, clone IH6, 1:10), anti-canine CD45 (Bio-rad, clone YKIX716.13, 1:10) and anti-human CD117 (BD Bioscience, clone YB5.B8, 1:10). Isotype controls were mouse IgG1 for CD34, CD29 and CD117 (BD Bioscience, clone MOPC-21, 1:10), rat IgG2b for CD90, CD45 and CD44 (eBioscience, clone eB149/10H5, 1:10) and rat IgG2a for CD105 (BD Biosciences, clone R35-95, 1:10). Antibodies were conjugated with R-phycoerythrin (RPE).

Flow cytometry

Samples were acquired in polystyrene FACS tubes on a BD FACS Calibur flow cytometer (BD Bioscience). The instrument was calibrated using CaliBRITE 3 colour FACS Comp beads (BD Bioscience) before acquiring and analysing each set of samples using CellQuest Pro software (BD biosciences). Unlabelled cells were acquired in order to set the forward and side scatter parameters to centre the cell population on the scatter plot. Fluorescence intensity was adjusted to set the unlabelled cells within 10^0 - 10^1 on the log scale axis. Cells were then acquired with an event count set to a total of 1 x 10^4 events. Data was analysed using FlowJo software (FlowJo, LLC). Further details are provided in MIFlowCyt (Supporting Information).

Population doubling time

Freshly prepared CDCs and MSCs (non-cryopreserved), and cryopreserved CDCs were assessed for growth kinetics using a population doubling time protocol (PDT) as

previously described (35). Cryopreserved cells were expanded for 3-5 days in tissue culture vessels as described above prior to the PDT protocol. Briefly, cells were detached from culture vessels using 0.25% trypsin, pelleted and counted by Trypan blue dye exclusion. 1 x 10^4 cells suspended in CEM (CDCs) or MSCM (MSCs) were plated per well, in 6-well plates, in triplicate for each cell type and each time point. Cells were detached with trypsin every 3-4 days for two weeks to perform cell counts. The doubling time was calculated according to the formula PDT = $\ln(N/N_0)/\ln 2$ where N was the final cell number and N_0 was the cell number at the beginning of the logarithmic increase.

Clonal growth assay

CDCs were trypsinised from culture vessels, counted and plated at very low density (20 cells/cm^2) on fibronectin coated 25cm^2 flasks. After 24 h individual cells were visualised on an Olympus inverted microscope (model CKX415F; Olympus Corporation). The culture vessel was observed daily for 10 days to identify the formation of colonies. Cells were discounted from analysis if more than one cell was present in the field of view of a low power objective lens (4 x magnification objective) at the start of the culture period. Images were captured with a colour digital camera (GT Vision Ltd.). Colony size was measured using ImageJ software version 1.50i (National Institute of Health).

Sphere size assessment

To assess the diameter of spheres formed from fresh CDCs and cryopreserved CDCs, cells were seeded at a density of 1 x 10^5/cm^2 on an ULA surface. The spheres formed were tracked with culture time and sphere number and diameter measured at 5 days

using ImageJ software. These parameters were compared to primary spheres that were formed by fresh CDCs at the same time point as detailed above in the preparation of cardiosphere-derived cells section.

Differentiation capacity of CDCs and MSCs

MSCs were induced to differentiate towards osteogenic, adipogenic (26-28) or smooth muscle (14) lineages as previously reported.

Osteogenic differentiation

MSCs were plated in 6-well plates (5,000 cell/cm^2) and cultured to 80% confluence before induction. Osteogenic induction medium consisted of DMEM with 10% FBS supplemented with dexamethasone (100nM), ascorbic acid (0.2mM) and β-glycerophosphate (10mM) (all from Sigma-Aldrich) with P/S. Medium was changed every 2-3 days. After 14 days of induction, extracellular calcium deposits were assessed using 2% Alizarin Red S (Sigma-Aldrich) staining at pH 4.3.

Adipogenic differentiation

MSCs were plated in 6-well plates (8,000 cell/cm^2) and cultured to 90-100% confluence before induction. Induction wells were subjected to alternating cycles of inductive medium (72 h) followed by maintenance medium (24 h) repeated 6 times. Inductive medium consisted of DMEM with 10% FBS supplemented with dexamethasone (1μM), 1% insulin, indomethacin (100μM), 3-isobutyl-1-methylxanthine (100μM) (all Sigma-Aldrich) with P/S. Oil-Red-O staining was used to assess intracytoplasmic lipid accumulation.

Smooth muscle and endothelial differentiation

Fresh CDCs, MSCs and cryopreserved CDCs were seeded onto fibronectin-coated Nunc Lab-Tek chamber slides (Thermo Fisher Scientific), allowed to reach 80% confluence and subjected to differentiation media for 12-13 days. Smooth muscle differentiation media consisted of IMDM with 1% L-glutamine, 1% P/S and 10ng/mL platelet-derived growth factor-β (PDGF-β, Preprotech; 100-14B). Endothelial differentiation media consisted of IMDM with 1% L-glutamine, 1% P/S and 50ng/mL vascular endothelial growth factor (VEGF, Preprotech; 100-20A). Immunocytochemistry was performed to assess formation of actin fibres or expression of von Willebrand factor (vWF).

Cardiomyocyte differentiation

Following monolayer culture, fresh CDCs and cryopreserved CDCs were dissociated and seeded at a density of 1 x $10^5/cm^2$ on either 24 or 6 well plates on a cell-repellent surface (Greiner Bio One) to form secondary cardiospheres. Once spheres had formed (3-5 days), media in inductive wells was changed to Cardiomyocyte Differentiation Kit media according to the manufacturers instructions (Thermo Fisher Scientific) and continued for 12-14 days. Next, spheres were harvested and attached to FBS-coated chamber slides for 18 h. Expression of cardiac troponin T (cTNT) was assessed by immunocytochemistry. Expression of cTNT was also assessed on individual cells as described for smooth muscle and endothelial differentiation.

Immunocytochemistry

Following termination of differentiation, cells were fixed in 4% PFA for 10 min then blocked and permeabilized in protein block solution (DAKO) containing 1% saponin (Sigma-Aldrich) for 1.5 h. Cells were incubated at 4°C with a primary antibody for 1 h then secondary antibodies for 1 h. The primary antibodies used were: monoclonal mouse anti-cardiac troponin T (Abcam, clone 1C11; 1:500 dilution), mouse anti-smooth muscle actin (Sigma-Aldrich, clone 1A4; 1:200) and polyclonal rabbit anti-von Willebrands factor (Abcam, 1:400). Fluorescein isothiocyanate (FITC) labelled secondary antibodies were purchased from Abcam (polyclonal goat anti-mouse IgG, 1:500) and Biolegend (polyclonal donkey anti-rabbit IgG, 1:250). Control slides consisted of unstained cells, undifferentiated cells and secondary antibody only stained slides. Slides were mounted with Vectashield containing 4', 6-diamidino-2-phenylindole (DAPI) (Vector Laboratories Ltd). Cells were visualised with an Olympus BX60 microscope (Olympus Corporation) equipped with a CoolLED pE-2 fluorescence illumination system (CoolLED Ltd.) and images captured using a QImaging QICAM digital camera.

Statistical analysis

GraphPad Prism 7 software (GraphPad Software Inc. CA, USA) was used for statistical analysis. Data was assessed for normality. All data is presented as the mean ± SEM unless stated otherwise. Comparisons between two independent samples were performed using student's two-tailed T-test and between three or more groups using one-way ANOVA with post-hoc Tukey analysis. A P value of < 0.05 was considered significant.

Results

Cardiosphere formation

CDCs were isolated and expanded from dogs (n=5) of different breeds or of non-pedigree origin. Donor characteristics are summarised in supplementary table 1 (Table S1). Within 5-7 days a stromal-like monolayer of cells emerged from the explants above which phase-bright cells migrated (Fig. 1A). The phase-bright cells formed spheres (Fig. 1B). Early passage CDCs showed a heterogeneous population of cell morphologies consisting of both long spindle shaped cells and rounded cells (Fig. 1C and D). CDCs had a post-cryopreservation viability of 95-98% after being frozen for 3 months and could be further expanded in monolayer culture on fibronectin-coated flasks. Culture expanded cells showed a similar heterogeneous morphology (Fig. 1E). By comparison MSCs prepared from adipose tissue showed typical spindle shaped cells, which were homogeneous in morphology (Fig. 1F).

Cardiosphere characteristics

Both cryopreserved and non-cryopreserved CDCs were able to readily form into secondary cardiospheres when plated onto a low attachment surface. The diameter of primary, secondary and cryopreserved cardiospheres was compared. Secondary spheres formed by fresh CDCs were 20% smaller than primary spheres (Fig. 2A; $P < 0.0001$). Strikingly, the spheres formed by cryopreserved cells were approximately three times larger than those formed from fresh CDCs (Fig. 2A; $P < 0.0001$).

Population doubling and cloning potential

The cloning potential and growth kinetics were assessed for CDCs prior to and after cryopreservation. The population doubling time was similar between the two groups (Fig. 2B; fresh versus cryopreserved; 57.13 ± 5.27 h versus 48.94 ± 9.55 h, $P = 0.71$). As a comparison, canine MSCs had a significantly faster population doubling time compared to both fresh and cryopreserved CDC (Fig. 2B; 30.46 h, $P < 0.05$). There was no significant difference in the diameter of clonal colonies between the two groups by day 7 (Fig. 2C; fresh versus cryopreserved; 1.30 ± 0.19 mm versus 1.20 ± 0.13 mm, $P = 0.73$). Both cell populations were able to form clonal colonies from single cells when plated at very low density (Fig. 2D).

Multipotency of CDCs and MSCs

When fresh and cryopreserved CDCs were placed into suspension culture to form secondary cardiospheres, they expressed high levels of troponin T within their cytoplasm following induction with a cardiomyocyte medium (Fig. 3A-I). In addition, single plated CDCs showed cytoplasmic troponin T staining that was mostly disorganised (Fig. 3J), but a small number of cells demonstrated early fibre alignment and striation (Fig. 3K). Both fresh and cryopreserved CDCs also demonstrated capacity for differentiation towards lineages of endothelium (positive expression of vWF) and smooth muscle (positive expression of α-smooth muscle actin, Fig. 3L-Q). MSCs also differentiated into a smooth muscle phenotype when induced with PDGF-β and expressed smooth muscle actin (Fig. 3R and S) and showed positive staining for Alizarin Red S and Oil Red O following induction in osteogenic or adipogenic medium, respectively, when compared to control cells (Fig. 4A-D).

Surface marker expression profile

Flow cytometry analysis showed fresh CDCs consisted of a high proportion of $CD105^+$ (89.0% ± 4.98) and $CD44^+$ (99.68% ± 0.13) cells, low proportions of $CD90^+$ (23.36% ± 9.78), $CD117^+$ (13.17% ± 8.67), $CD29^+$ (2.92% ± 2.46) cells and a negligible proportion of $CD45^+$ cells (0.005% ± 0.003, Fig. 5A-F). In contrast MSCs showed a high proportion of $CD90^+$ (99.60% ± 0.30), $CD44^+$ (99.85% ± 0.05) and $CD105^+$ (76.55% ± 22.35) cells and a small fraction of $CD34^+$ cells (1.80% ± 1.76). $CD117^+$ (0.92% ± 0.34), $CD45^+$ (0.015% ± 0.005) and $CD29^+$ (0.57% ± 0.46) cells represented a very small fraction (Fig. 5M-R). Interestingly, the percentage of $CD34^+$ cells was variable with passage number with low percentages in low passage CDCs (P1-2; 7.18% ± 4.03) but increased to moderate and high percentages with further passaging (P4-6; 59.75% ± 3.45, P = 0.003, Fig. 6A-C), with high percentages following cryopreservation (79.35% ± 4.85, Fig. 6D). This was in contrast to the proportion of $CD90^+$ cells, which was higher in unpassaged cells (P0; 42.55% ± 13.65) but decreased in P4-5 (15.04% ± 9.77, P = 0.03, Fig. 6 E-G). The $CD90^+$ fraction was low in CDCs following cryopreservation (3.03% ± 1.41, Fig. 6H). Other markers (CD105, CD44, CD45, CD117 and CD29) exhibited a similar expression profile between fresh and cryopreserved CDCs.

Discussion

In this study we derived CDCs from multiple donor animals for characterisation prior to and following cryopreservation, since to the authors knowledge the effect of freezing on CDCs has not been assessed in any species. Understanding the effect of cryopreservation on these cells is vital for conducting clinical trials using frozen CDCs. The effect of cryopreservation is well characterised for MSCs (37,38); however, previous attempts in our laboratory to freeze canine cardiac stem cells suggested they may be more labile than MSCs to cryopreservation. We utilised atrial tissue as previous reports indicated a higher number of c-Kit$^+$ cells present within the atria and therefore potentially a greater number of cardiac stem cells may be obtained compared to the ventricle (17,24). Atrial tissue has also been used previously to isolate canine cardiac stem cells (33). We demonstrate for the first time that cryopreservation of canine CDCs does not affect their vital stem cell characteristics. Firstly, there were no significant differences in clonal growth and population doubling characteristics suggesting that CDCs tolerate freezing. The ability of CDCs to differentiate was also unaffected since they were able to express α-smooth muscle actin, von Willebrand factor and troponin T indicating commitment to the smooth muscle, endothelial and cardiomyocyte lineages, respectively, as reported by others for fresh cells (25,31). Furthermore, fresh and cryopreserved CDCs demonstrated cardiomyogenic potential following secondary sphere formation and culture in the presence of cardiomyocyte differentiation media. Cytological staining on individual cells shows mostly an immature troponin organisation, although a small fraction of cells demonstrated a more complex organisation, characterized by the emergence of a striated pattern.

Conversely, the process of cryopreservation did alter the proportions of certain cell surface markers. Specifically, the $CD34^+$ fraction was increased after culture of cryopreserved CDCs. CD34, a transmembrane phosphoglycoprotein, is found on a diverse range of cells and appears to have multiple functions. It has been associated with cell-cell adhesion and highly proliferative cells (39–41). CD34 is often used as an exclusion criteria for MSCs (42), however a more recent literature review indicates its presence on some MSC populations (specifically adipose derived MSCs) and is expressed by a diverse range of other progenitor cells (43). The higher proliferative capacity of the $CD34^+$ population (34-36) may explain the increase we observed with passage number and following cryopreservation. $CD34^+$ cells also appear highly tolerant to freezing when compared to other nucleated cell types and therefore may have better survival in the heterogeneous CDC population (44). This may have clinical relevance as experiments in animal models of myocardial infarction using $CD34^+$ purified cell populations showed an increased cellular persistence within the myocardium and showed positive effects on heart function (45,46).

In comparison with other species, early passage (P2) human CDCs exhibit a similar $CD34^+$ population (approximately 10%) (47). However, another study reported fewer $CD34^+$ cells (1%) in human CDCs of undefined passage number (48). It has also been noted that increasing media serum content from 10% to 20% increases the $CD34^+$ population from 0.9% to 7.5% (31). Cardiac progenitor cells grown directly from rat heart

explants (without the cardiosphere step) declined in their $CD34^+$ population over a culture period of 35 days (23).

Furthermore there were varying proportions of $CD90^+$ cells, which was both inter-donor (the variability between donors) and intra-donor dependent (the variability within a donor, dependent on culture conditions). The $CD90^+$ fraction also decreased following cryopreservation and increasing passage number of fresh cells. CD90 (Thymocyte antigen-1; Thy-1) is a commonly used marker for MSCs in all reported species, including canines (35,49–51). The $CD90^+$ population in our CDC preparations exists as a small fraction, as noted by others (20,29,45). Our finding that the CD90 population can be manipulated by passaging or cryopreservation may have clinical implications as this population appeared to reduce the therapeutic efficacy of CDCs in a rodent model of myocardial infarction (24).

Cryopreserved CDCs formed cardiospheres that were approximately three times larger than their fresh counterparts. This may be due to the higher $CD34^+$ fraction increasing the cell-cell adhesion efficiency. Alternatively this may be an integrin dependent interaction as this has previously been shown to significantly increase the adherence and cell-cell binding in MSCs (52). This may be clinically relevant as the larger size could predispose them to arteriole blockage and subsequent tissue ischemia. Sphere size would therefore need to be controlled by the use of aggregation wells (53).

In comparison with other species, canine CDCs exhibit remarkable phenotypic similarities to mouse, rat, human and porcine cells (21,22,28,54,55). As we elucidated in the introduction, canines are a unique naturally occurring model for non-ischemic cardiomyopathy in humans, specifically ARVC (8,10,56). The effect of cryopreservation on human CDCs is poorly understood; therefore given the similarities with canine cells the present study also provides vital translational information to the human field. Also phenotypically the sphere size formed from fresh cells is similar to reports in other species (21,31), conversely the large spheres from cryopreserved cells has not been noted previously. There are other notable differences. Firstly, differentiation of canine CDCs to functioning cardiomyocytes appears challenging. Methods attempting to translate mouse and rat differentiation protocols to canine cells have proved only partially successful (25,33). We also found similar difficulties in using cardiac differentiation media designed for mouse and human iPSCs. Additionally the c-Kit$^+$ proportion in our atrial derived CDCs was higher than that reported in mouse, human and canine ventricular derived CDCs (22,23,25,30,31). C-Kit$^+$ cells have been reported to be localised in areas within the heart with low haemodynamic stress, such as the atria in humans (17,18,57). The location of c-Kit expressing cells in the canine heart has not been described but the tissue compartment (atria) source likely explains the greater c-Kit$^+$ population in our CDCs. Previous studies with canine CDCs have examined ventricular tissue from a single donor (25,30) which limits the comparative interpretation with our study.

In conclusion, we conduct for the first time phenotypic analysis of CDCs prior to and following cryopreservation. Our most important finding is that the key stem characteristics

of these cells are unchanged by this process. Changes were noted in the populations of cells expressing CD34 and CD90; however, the clinical significance of this is unknown, but based on previous literature could be beneficial. Our results show promise for the creation of cryopreserved cell banks for usage in future clinical trials.

Conflict of interest

The authors have declared no conflict of interest.

Acknowledgments

This study was funded by The PetPlan Charitable Trust (Project number: 214-252). Royal Veterinary College manuscript approval number CSS_01545.

Literature Cited

1. Egenvall A, Bonnett BN, Häggström J. Heart Disease as a Cause of Death in Insured Swedish Dogs Younger Than 10 Years of Age. J Vet Intern Med. 2006;20(4):894–903.
2. Simpson S, Dunning MD, Brownlie S, Patel J, Godden M, Cobb M, et al. Multiple Genetic Associations with Irish Wolfhound Dilated Cardiomyopathy. Hindawi Publishing Corporation; 2016;2016:6374082.
3. Simpson S, Edwards J, Ferguson-Mignan TFN, Cobb M, Mongan NP, Rutland CS. Genetics of human and canine dilated cardiomyopathy. Int J Genomics. Hindawi Publishing Corporation; 2015;2015:204823.
4. Simpson S, Edwards J, Emes RD, Cobb MA, Mongan NP, Rutland CS. A predictive model for canine dilated cardiomyopathy-a meta-analysis of Doberman Pinscher data. PeerJ. 2015;3:e842.
5. Meurs KM, Stern JA, Sisson DD, Kittleson MD, Cunningham SM, Ames MK, et al. Association of dilated cardiomyopathy with the striatin mutation genotype in boxer dogs. J Vet Intern Med. 2013;27(6):1437–40.
6. Mausberg TB, Wess G, Simak J, Keller L, Drögemüller M, Drögemüller C, et al. A locus on chromosome 5 is associated with dilated cardiomyopathy in doberman pinschers. PLoS One. 2011;6(5):5–10.
7. Tidholm A, Jönsson L, Jonsson L. Histologic Characterization of Canine Dilated Cardiomyopathy. Vet Pathol. 2005;42(1):1–8.

8. Basso C, Fox PR, Meurs KM, Towbin JA, Spier AW, Calabrese F, et al. Arrhythmogenic Right Ventricular Cardiomyopathy Causing Sudden Cardiac Death in Boxer Dogs: A New Animal Model of Human Disease. Circulation. 2004;109(9):1180–5.
9. Vila J, Pariaut R, Moïse NS, Oxford EM, Fox PR, Reynolds CA, et al. Structural and molecular pathology of the atrium in boxer arrhythmogenic right ventricular cardiomyopathy. J Vet Cardiol. 2017 Feb;19(1):57–67.
10. Oxford EM, Danko CG, Fox PR, Kornreich BG, Moïse NS. Change in β-Catenin localization suggests involvement of the canonical wnt pathway in boxer dogs with arrhythmogenic right ventricular cardiomyopathy. J Vet Intern Med. 2014;28(1):92–101.
11. Yamada N, Kitamori T, Kitamori F, Ishigami K, Iwanaga K, Itou T, et al. Arrhythmogenic right ventricular cardiomyopathy coincided with the cardiac fibrosis in the inner muscle layer of the left ventricular wall in a boxer dog. J Vet Med Sci. 2015;77(10):1299–303.
12. Meurs KM, Stern JA, Reina-Doreste Y, Spier AW, Koplitz SL, Baumwart RD. Natural History of Arrhythmogenic Right Ventricular Cardiomyopathy in the Boxer Dog: A Prospective Study. J Vet Intern Med. 2014;28(4):1214–20.
13. Saffitz JE. Desmosome mutations in arrhythmogenic right ventricular cardiomyopathy important insight but only part of the picture. Circ Cardiovasc Genet. 2009;2(5):415–7.
14. Wess G, Schulze A, Butz V, Simak J, Killich M, Maeurer J, et al. Prevalence of Dilated Cardiomyopathy in Doberman Pinschers in Various Age Groups. J Vet

Intern Med. 2010;(24):533–8.

15. Nadal-Ginard B, Kajstura J, Leri A, Anversa P. Myocyte death, growth, and regeneration in cardiac hypertrophy and failure. Circ Res. 2003;92(2):139–50.
16. Condorelli G, Borello U, De Angelis L, Latronico M, Sirabella D, Coletta M, et al. Cardiomyocytes induce endothelial cells to trans-differentiate into cardiac muscle: implications for myocardium regeneration. Proc Natl Acad Sci U S A. 2001;98(19):10733–8.
17. He JQ, Vu DM, Hunt G, Chugh A, Bhatnagar A, Bolli R. Human cardiac stem cells isolated from atrial appendages stably express c-kit. PLoS One. 2011;6(11).
18. Hosoda T. C-kit-positive cardiac stem cells and myocardial regeneration. Am J Cardiovasc Dis. 2012;2(1):58–67.
19. Genead R, Danielsson C, Wärdell E, Kjaeldgaard A, Westgren M, Sundström E, et al. Early first trimester human embryonic cardiac Islet-1 progenitor cells and cardiomyocytes: Immunohistochemical and electrophysiological characterization. Stem Cell Res. Elsevier B.V.; 2010;4(1):69–76.
20. Matsuura K, Nagai T, Nishigaki N, Oyama T, Nishi J, Wada H, et al. Adult Cardiac Sca-1-positive Cells Differentiate into Beating Cardiomyocytes. J Biol Chem. 2004;279(12):11384–91.
21. Messina E, De Angelis L, Frati G, Morrone S, Chimenti S, Fiordaliso F, et al. Isolation and expansion of adult cardiac stem cells from human and murine heart. Circ Res. 2004;95(9):911–21.
22. Chimenti I, Smith RR, Li TS, Gerstenblith G, Messina E, Giacomello A, et al. Relative roles of direct regeneration versus paracrine effects of human

cardiosphere-derived cells transplanted into infarcted mice. Circ Res. 2010;106(5):971–80.

23. Davis DR, Kizana E, Terrovitis J, Barth AS, Zhang Y, Smith RR, et al. Isolation and expansion of functionally-competent cardiac progenitor cells directly from heart biopsies. J Mol Cell Cardiol. Elsevier Ltd; 2010;49(2):312–21.
24. Cheng K, Ibrahim A, Hensley MT, Shen D, Sun B, Middleton R, et al. Relative Roles of CD90 and c-Kit to the Regenerative Efficacy of Cardiosphere-Derived Cells in Humans and in a Mouse Model of Myocardial Infarction. J Am Heart Assoc. 2014;3(5):e001260.
25. Hensley MT, de Andrade J, Keene B, Meurs K, Tang J, Wang Z, et al. Cardiac regenerative potential of cardiosphere-derived cells from adult dog hearts. J Cell Mol Med. 2015;19(8):1805–13.
26. Johnston P V, Sasano T, Mills K, Evers R, Lee S, Smith RR, et al. Engraftment, differentiation and functional benefit of autologous cardiosphere-derived cells in a porcine ischemic cardiomyopathy. Circulation. 2009;(120):1075–83.
27. Kanazawa H, Tseliou E, Dawkins JF, De Couto G, Gallet R, Malliaras K, et al. Durable benefits of cellular postconditioning: long-term effects of allogeneic cardiosphere-derived cells infused after reperfusion in pigs with acute myocardial infarction. J Am Heart Assoc. 2016;5(2):1–16.
28. Makkar RR, Smith RR, Cheng K, Malliaras K, Thomson LEJ, Berman D, et al. Intracoronary cardiosphere-derived cells for heart regeneration after myocardial infarction (CADUCEUS): A prospective, randomised phase 1 trial. Lancet. Elsevier Ltd; 2012;379(9819):895–904.

29. Malliaras K, Makkar RR, Smith RR, Cheng K, Wu E, Bonow RO, et al. Intracoronary cardiosphere-derived cells after myocardial infarction: Evidence of therapeutic regeneration in the final 1-year results of the CADUCEUS trial (CArdiosphere-derived aUtologous stem CElls to reverse ventricular dysfunction). J Am Coll Cardiol. 2014;63(2):110–22.

30. Hensley MT, Tang J, Woodruff K, Defrancesco T, Tou S, Williams CM, et al. Intracoronary allogeneic cardiosphere-derived stem cells are safe for use in dogs with dilated cardiomyopathy. J Cell Mol Med. 2017;XX(X):1–10.

31. Davis DR, Zhang Y, Smith RR, Cheng K, Terrovitis J, Malliaras K, et al. Validation of the cardiosphere method to culture cardiac progenitor cells from myocardial tissue. PLoS One. 2009;4(9):e7195.

32. Cho H-J, Lee H-J, Youn S-W, Koh S-J, Won J-Y, Chung Y-J, et al. Secondary sphere formation enhances the functionality of cardiac progenitor cells. Mol Ther. 2012;20(9):1750–66.

33. Hodgkiss-Geere HM, Argyle DJ, Corcoran BM, Whitelaw B, Milne E, Bennett D, et al. Characterisation and cardiac directed differentiation of canine adult cardiac stem cells. Vet J. Elsevier Ltd; 2012;191(2):176–82.

34. Kisiel a H, McDuffee L a, Masaoud E, Bailey TR, Esparza Gonzalez BP, Nino-Fong R. Isolation, characterization, and in vitro proliferation of canine mesenchymal stem cells derived from bone marrow, adipose tissue, muscle, and periosteum. Am J Vet Res. 2012;73(8):1305–17.

35. Screven R, Kenyon E, Myers MJ, Yancy HF, Skasko M, Boxer L, et al. Immunophenotype and gene expression profile of mesenchymal stem cells

derived from canine adipose tissue and bone marrow. Vet Immunol Immunopathol. Elsevier B.V.; 2014;161(1–2):21–31.

36. Takemitsu H, Zhao D, Yamamoto I, Harada Y, Michishita M, Arai T. Comparison of bone marrow and adipose tissue-derived canine mesenchymal stem cells. BMC Vet Res. 2012;8:150.

37. Martinello T, Bronzini I, Maccatrozzo L, Mollo A, Sampaolesi M, Mascarello F, et al. Canine adipose-derived-mesenchymal stem cells do not lose stem features after a long-term cryopreservation. Res Vet Sci. Elsevier Ltd; 2011;91(1):18–24.

38. Marquez-Curtis LA, Janowska-Wieczorek A, McGann LE, Elliott JAW. Mesenchymal stromal cells derived from various tissues: Biological, clinical and cryopreservation aspects. Cryobiology. Elsevier Inc.; 2015;71(2):181–97.

39. Healy L, May G, Gale K, Grosveld F, Greaves M ET. The stem cell antigen CD34 functions as a regulator of hemopoietic cell adhesion. Proc Natl Acad Sci U S A. Proc Natl Acad Sci; 1995;92:12240–4.

40. Huss R. Isolation of primary and immortalized CD34-hematopoietic and mesenchymal stem cells from various sources. Stem Cells. 2000;18(1):1–9.

41. Servida F, Soligo D, Caneva L, Bertolini F, Harven E De, Campiglio S, et al. Functional and Morphological Characterization of Immunomagnetically Selected CD34 + Hematopoietic Progenitor Cells. 1996;430–8.

42. Dominici M, Le Blanc K, Mueller I, Slaper-Cortenbach I, Marini F, Krause D, et al. Minimal criteria for defining multipotent mesenchymal stromal cells. The International Society for Cellular Therapy position statement. Cytotherapy. Elsevier; 2006;8(4):315–7.

43. Sidney LE, Branch MJ, Dunphy SE, Dua HS, Hopkinson A. Concise Review : Evidence for CD34 as a Common Marker for Diverse Progenitors. Stem Cells. 2014;32:1380–9.

44. Moezzi L, Pourfathollah AA, Alimoghaddam K, Soleimani M, Ardjmand AR. The effect of cryopreservation on clonogenic capacity and in vitro expansion potential of umbilical cord blood progenitor cells. Transplant Proc. 2005;37(10):4500–3.

45. Wang J, Zhang S, Rabinovich B, Bidaut L, Soghomonyan S, Alauddin MM, et al. Human CD34+ cells in experimental myocardial infarction: Long-term survival, sustained functional improvement, and mechanism of action. Circ Res. 2010;106(12):1904–11.

46. Botta R, Gao E, Stassi G, Bonci D, Pelosi E, Zwas D, et al. Heart infarct in NOD-SCID mice: therapeutic vasculogenesis by transplantation of human CD34+ cells and low dose CD34+KDR+ cells. FASEB J. 2004;18(12):1392–4.

47. Smith RR, Barile L, Cho HC, Leppo MK, Hare JM, Messina E, et al. Regenerative potential of cardiosphere-derived cells expanded from percutaneous endomyocardial biopsy specimens. Circulation. 2007;115(7):896–908.

48. Li TS, Cheng K, Malliaras K, Smith RR, Zhang Y, Sun B, et al. Direct comparison of different stem cell types and subpopulations reveals superior paracrine potency and myocardial repair efficacy with cardiosphere-derived cells. J Am Coll Cardiol. 2012;59(10):942–53.

49. Davies OG, Cooper PR, Shelton RM, Smith AJ, Scheven BA. Isolation of adipose and bone marrow mesenchymal stem cells using CD29 and CD90 modifies their capacity for osteogenic and adipogenic differentiation. J Tissue Eng. 2015;6:1–10.

50. Comparing the osteogenic potential of canine mesenchymal stem cells derived from adipose tissues, bone marrow, umbilical cord blood, and Wharton's jelly for treating bone defects. J Vet Sci. 2012;3(13):299–310.

51. Takemitsu H, Zhao D, Yamamoto I, Harada Y, Michishita M, Arai T. Comparison of bone marrow and adipose tissue-derived canine mesenchymal stem cells. BMC Vet Res. BMC Veterinary Research; 2012;8(1):150.

52. Clements LE, Garvican ER, Dudhia J, Smith RKW. Modulation of mesenchymal stem cell genotype and phenotype by extracellular matrix proteins. Connect Tissue Res. 2016;57(6):443–53.

53. Cho HJ, Lee HJ, Chung YJ, Kim JY, Cho HJ, Yang HM, et al. Generation of human secondary cardiospheres as a potent cell processing strategy for cell-based cardiac repair. Biomaterials. Elsevier Ltd; 2013;34(3):651–61.

54. Malliaras K, Li TS, Luthringer D, Terrovitis J, Cheng K, Chakravarty T, et al. Safety and efficacy of allogeneic cell therapy in infarcted rats transplanted with mismatched cardiosphere-derived cells. Circulation. 2012;125(1):100–12.

55. Poncelet AJ, Vercruysse J, Saliez A, Gianello P. Although pig allogeneic mesenchymal stem cells are not immunogenic in vitro, intracardiac injection elicits an immune response in vivo. Transplantation. 2007;83(6):783–90.

56. Vila J, Pariaut R, Moïse NS, Oxford EM, Fox PR, Reynolds CA, et al. Structural and molecular pathology of the atrium in boxer arrhythmogenic right ventricular cardiomyopathy. J Vet Cardiol. 2017;19(1):57–67.

57. Simpson DL, Mishra R, Sharma S, Goh SK, Deshmukh S, Kaushal S. A Strong Regenerative Ability of Cardiac Stem Cells Derived From Neonatal Hearts.

Circulation. 2015;33(4):395–401.

Figure legends

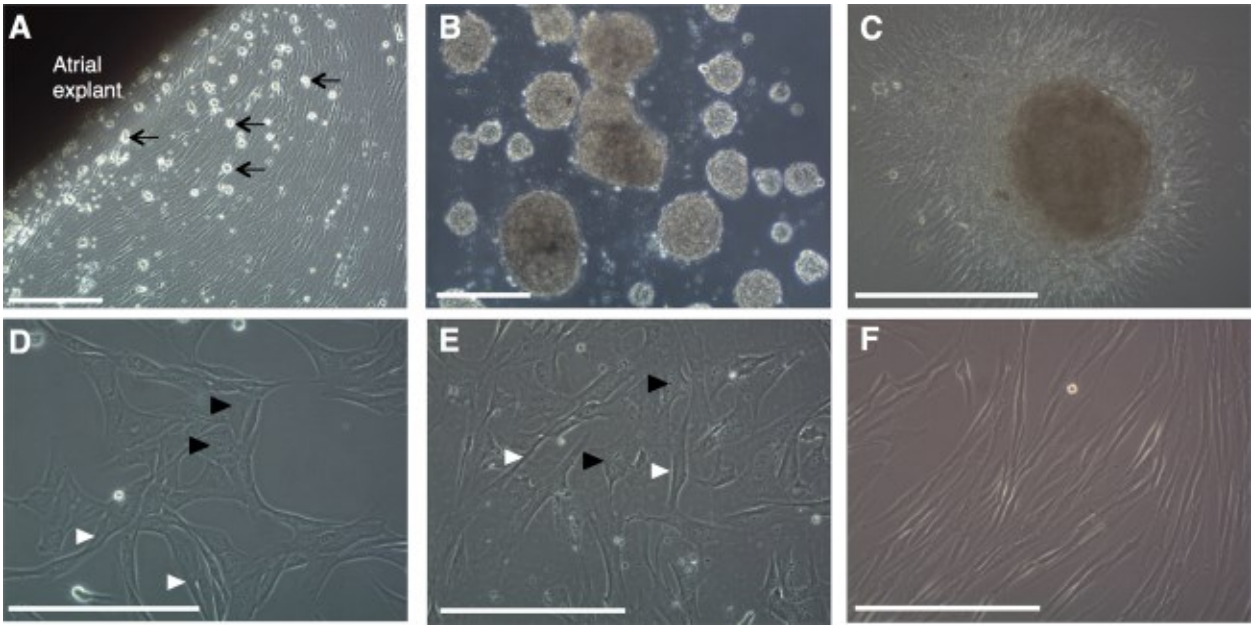

Figure 1: Representative photomicrographs showing the formation of cardiosphere-derived cells (CDCs) and mesenchymal stem cells (MSCs). Panel (A) stromal-like outgrowth cells from an atrial tissue explant with phase-bright cells (long arrows) migrating over the spindle like cell monolayer. The phase-bright cells were harvested and further grown in suspension culture to form cardiospheres (B). Heterogeneous sized cardiospheres were typically formed. Cardiospheres were collected by aspiration and seeded on fibronectin-coated tissue culture plastic to form cardiosphere-derived cells (CDCs) which are the fibronectin adherent population emerging from the cardiosphere (C) and shown at higher magnification (D). CDCs that were cultured following cryopreservation (E) had a similar morphology to fresh CDCs (D). The CDC population typically contained a mixture of spindle like cells (white arrows) among more rounded cells (black arrows). These are representative results for atrial tissue from five dogs. MSCs showed typical spindle like cell morphology (F). Scale bars = 250μm.

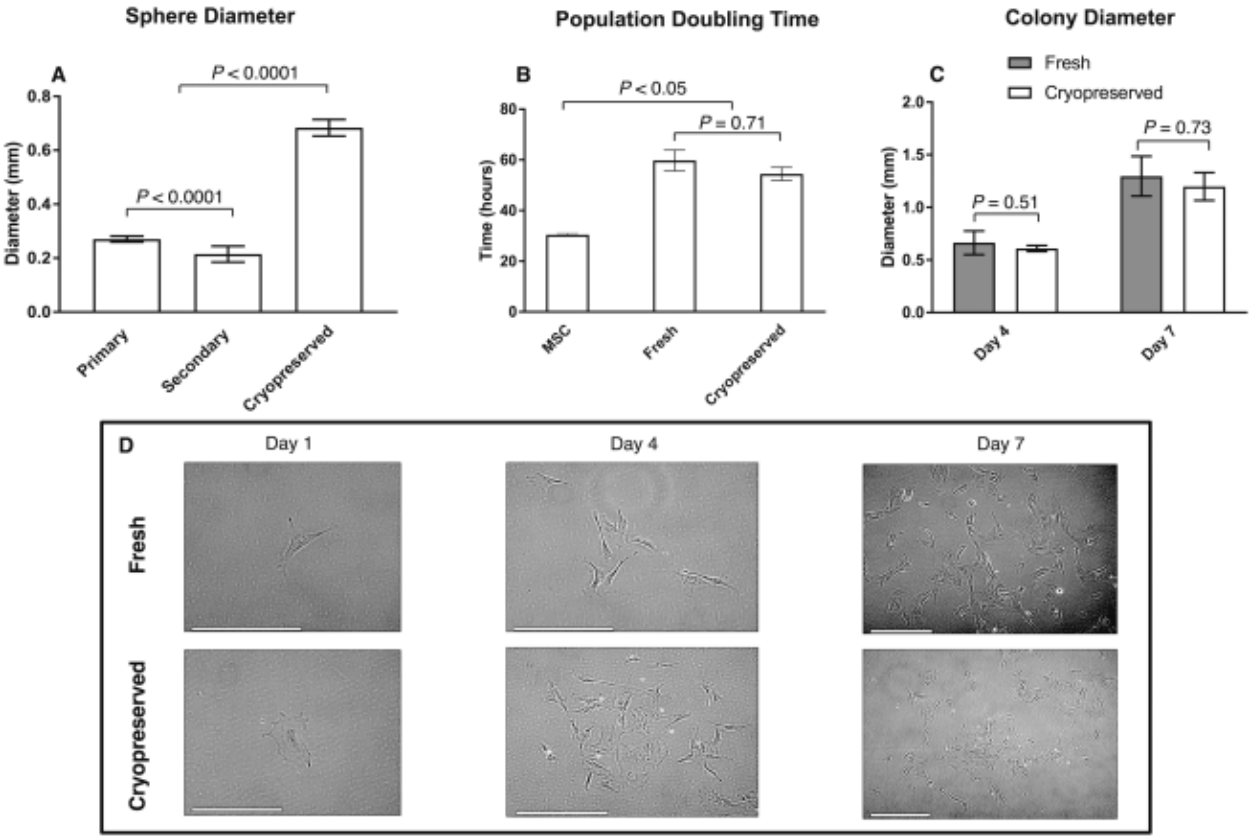

Figure 2: Comparison of growth characteristics of canine cardiosphere-derived cells (CDCs). (A) Sphere diameters of primary and secondary cardiospheres obtained from fresh cells and from cryopreserved cells. Secondary spheres were significantly smaller than primary spheres and spheres obtained from cryopreserved CDC were significantly larger than either primary or secondary spheres. (B) There was no significant difference in the PDT between fresh and cryopreserved cells but both were significantly slower compared to canine adipose MSCs. (C) Colony diameter for fresh and cryopreserved CDCs plated at low density. Colony size measurements shown were taken at days 4 and 7 and showed no significant difference between the two cell populations on either day. (D) Clonal expansion of CDCs from both fresh and cryopreserved cells. Scale bars = 250μm.

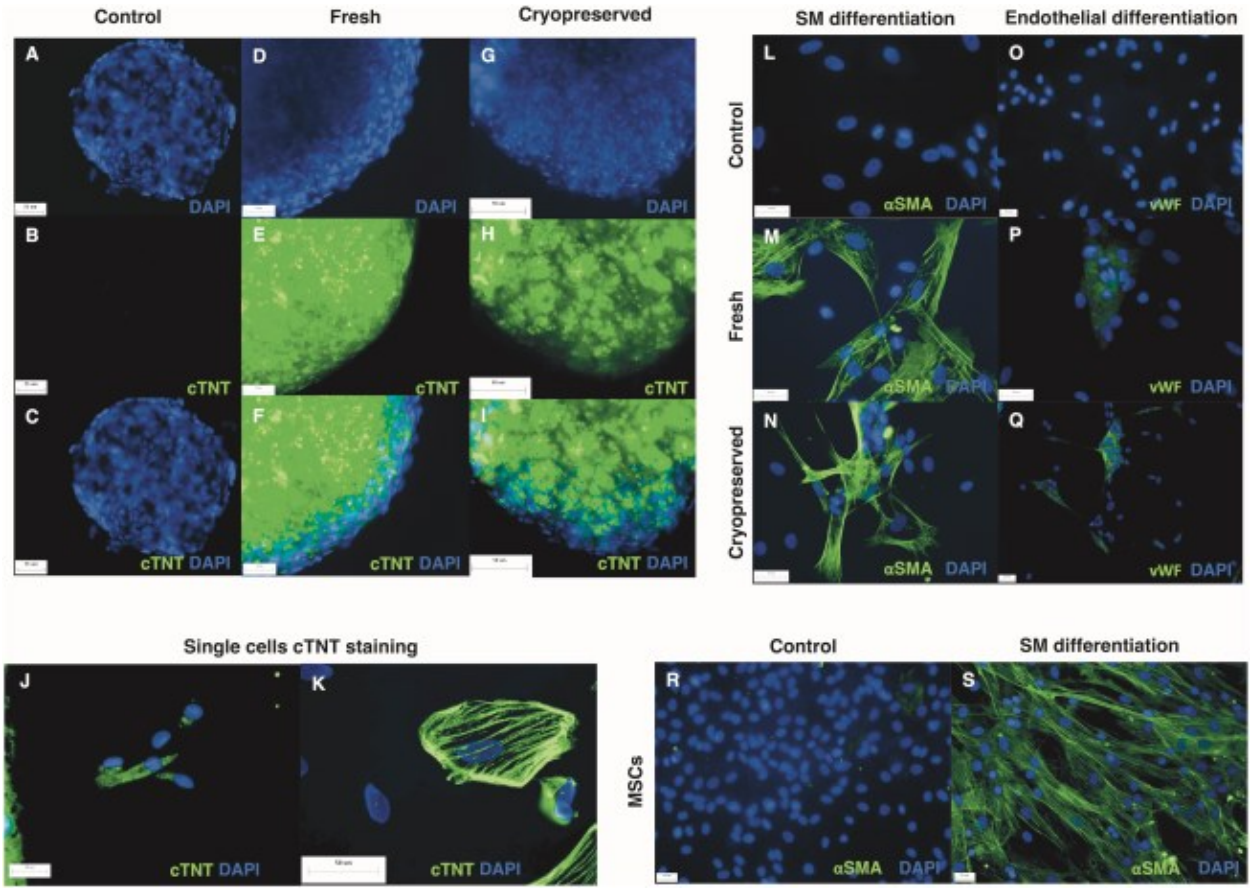

Figure 3: Cardiac, smooth muscle and endothelial differentiation. Fresh and cryopreserved canine cardiosphere-derived cells (CDCs) demonstrated expression of cardiac troponin T (cTNT, green fluorescence) following repeat sphere formation in the presence of cardiomyocyte differentiation medium (A-I). Individual CDCs for the majority showed disorganised cTNT protein (J), although a small number of cells showed an early-striated fibre pattern (K). CDCs were also able to differentiate towards a smooth muscle lineage as shown by expression of alpha-smooth muscle actin (α-SMA, green fluorescence) when compared to control cells (L and M), this ability was unaffected by cryopreservation (N). Expression of von Willebrand factor (vWF, green fluorescence) demonstrating a commitment to the endothelial lineage in fresh and cryopreserved cells (O-Q). MSCs showed marked up-regulation of α-SMA on induction when compared to

control cells (P and Q). Nuclei are counterstained with DAPI (blue fluorescence). Scale bars = 50μm (D-I and K) 25μm (other panels).

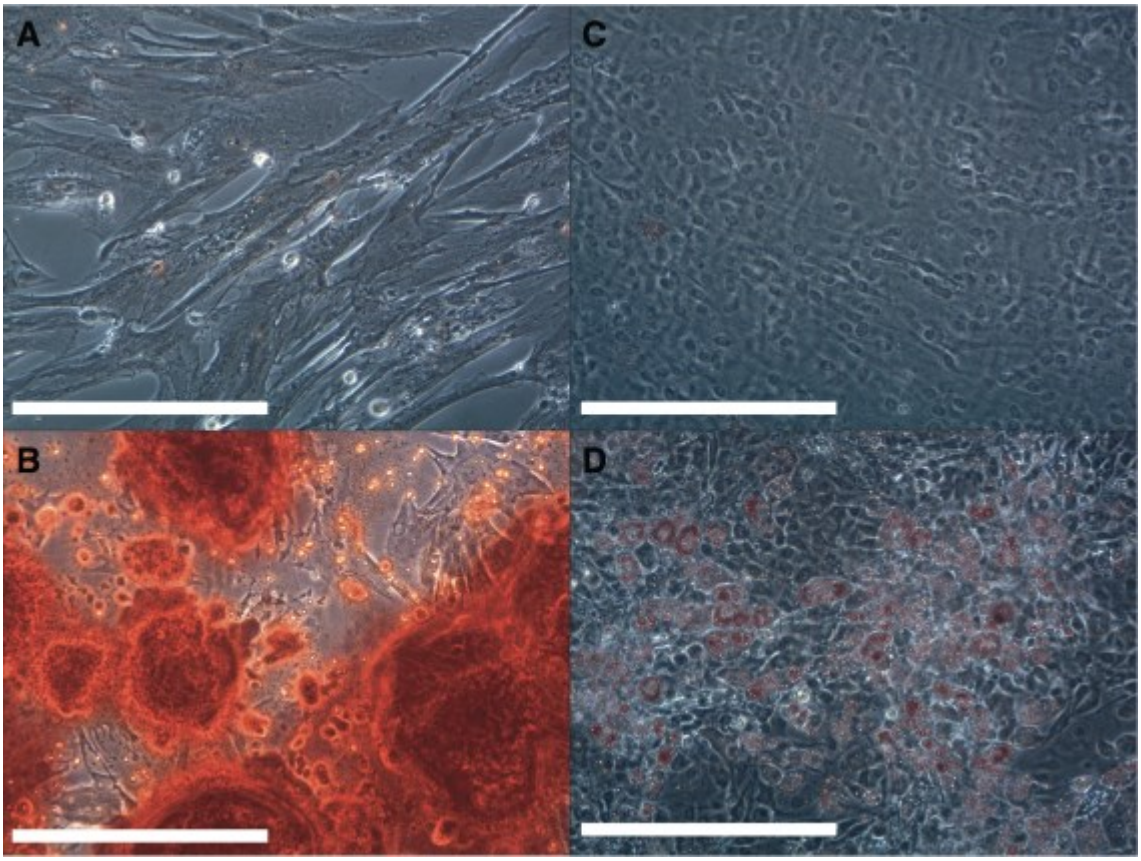

Figure 4: Adipogenic and osteogenic differentiation of mesenchymal stem cells (MSCs). Photomicrographs depicting Alizarin Red S staining for osteogenic differentiation: (A) control (non-induced) cells and (B) induced cells showing positive red staining for mineral deposition. Oil Red O staining for adipogenic differentiation: (C) control (non-induced) cells, (D) induced cells showing intracellular deposits of red stained oil droplets. Images are representative of differentiation of cells derived from five dogs. Scale bar = 250μm.

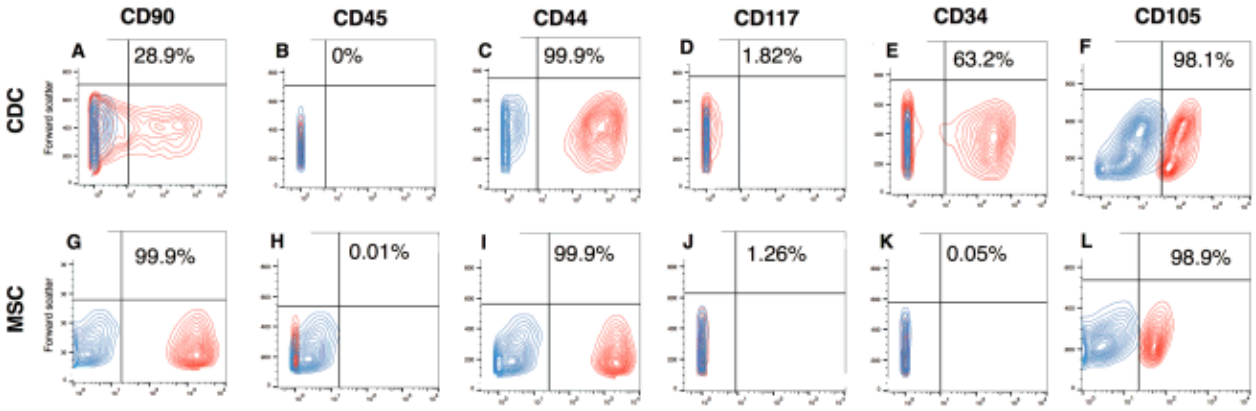

Figure 5: Flow cytometry contour plots for surface marker expression analysis of cardiosphere-derived cells (CDCs) and mesenchymal stem cells (MSCs). CDCs show intermediate proportions of $CD90^+$ cells (A), negligible $CD45^+$ cells (B), high proportion of $CD44^+$ cell (C), low numbers of $CD117^+$ cells (D), intermediate to high $CD34^+$ cell percentage (E) and high $CD105^+$ cell portion (F). MSCs showed a high percentage of $CD90^+$ cells (G), low proportion of $CD45^+$ cells (H), high $CD44^+$ proportion (I), negligible $CD117^+$ (J) and $CD34^+$ proportion (K) and a high $CD105^+$ proportion (L). Blue contours denote isotype control and red contours denote antibody labeled samples. Antibodies were R-PE conjugated.

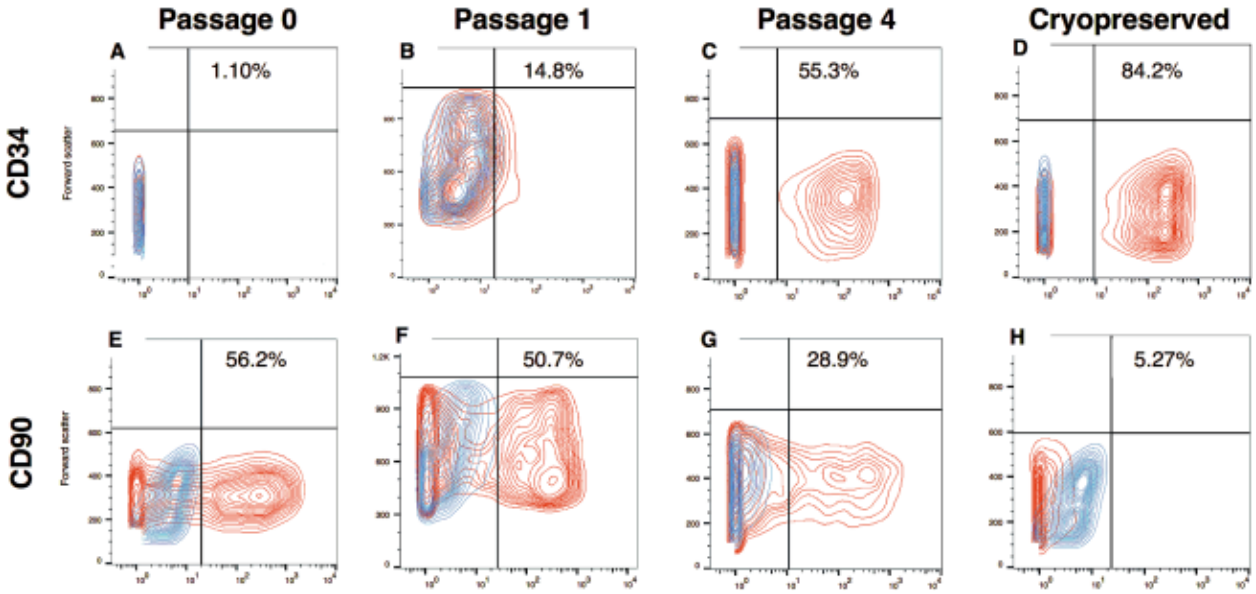

Figure 6: Flow cytometry comparing CD34 and CD90 expression on cardiosphere-derived cells (CDCs) at different passages and post-cryopreservation. $CD34^+$ cell were negligible in P0 cells (A; 1.1%) but increased from P1 to P4 (B and C, 14.8% and 55.3%). Cryopreserved cells showed a high $CD34^+$ proportion (D, 84.2%). Conversely the $CD90^+$ portion was reduced with passage number. P0 CDCs showed a high $CD90^+$ percentage (E, 56.2%), and 50.7% at P1 (F) and 28.9% at P4 (G). CD90 was absent in cryopreserved CDCs (H). Blue contours denote isotype control and red contours denote antibody labeled samples.